


 Cite this: *RSC Adv.*, 2026, 16, 8960

## Secondary metabolites from *Lobaria pulmonaria* (L.) Hoffm. target key metabolic enzymes: a novel strategy against multidrug-resistant tuberculosis

 Ha Thi Nguyen,<sup>†ab</sup> Vishnu Nayak Badavath,<sup>id c</sup> Siddhartha Maji,<sup>id d</sup> Haritha Polimati,<sup>id e</sup> Emmanuel Okello,<sup>f</sup> Richard A. Bunce,<sup>id d</sup> Nguyen Huy Thuan,<sup>ab</sup> Wan Mohd Nuzul Hakimi Wan Salleh<sup>id g</sup> and Vinay Bharadwaj Tatipamula<sup>id \*ab</sup>

Numerous cultures have traditionally utilised the foliose lichen *Lobaria pulmonaria* (L.) Hoffm. ("Oak Lung" or "Lungs of Oak" in English; family: Lobariaceae) as a Tuberculosis (Tb) treatment. The present study aimed to scientifically validate the folkloric use of *L. pulmonaria* in treating Tb by investigating its antimycobacterial profile against *Mycobacterium tuberculosis* H37Ra (*M.tb*) and six other MDR-Tb isolates. The preliminary results obtained from XRMA revealed the notable inhibitory activity of LP and Fraction (F)-3 against *M.tb*, displaying IC<sub>50</sub> values of 7.74 ± 0.27 and 6.26 ± 0.04 µg mL<sup>-1</sup>, respectively; followed by F2 (IC<sub>50</sub> value: 38.82 ± 0.34 µg mL<sup>-1</sup>) and F5 (IC<sub>50</sub> value: 46.69 ± 1.13 µg mL<sup>-1</sup>). The purification process of these bioactive fractions resulted in the identification of four known secondary metabolites: fukinanolide A, pinastric acid, stictic acid, and scrobiculin. Furthermore, the MICs from REMA showed that LP, stictic acid, and fukinanolide A have greater efficacy in controlling the growth of all six tested MDR-Tb isolates, compared to rifampicin. Notably, LP exhibited superior antimycobacterial activity against all six tested MDR strains as compared to all isolated compounds and rifampicin, possibly due to the synergistic effect of its metabolites. Furthermore, the IC<sub>50</sub> values of LP, stictic acid, and fukinanolide A on THP-1 macrophages were considerably higher than MICs against the tested mycobacterial strains, suggesting that THP-1 remained unaffected at concentrations effective against *M.tb* and MDR-Tb isolates. The deliberated SI ratio values indicated that LP, stictic acid, and fukinanolide A were more active and less toxic to MDR-Tb strains than rifampicin. The molecular docking studies on 1EA1, 4V1F and 3VIU revealed that fukinanolide A and stictic acid bind effectively and selectively to 3VIU (β-ketoacyl reductase FabG4), thereby conferring their anti-TB potential. The outcomes provide a validation for the traditional use of *L. pulmonaria* in Tb treatment, with stictic acid and fukinanolide A identified as key biomarkers. Hence, *L. pulmonaria* presented as a promising source for the development of novel drugs targeting against MDR-Tb.

 Received 7th August 2025  
 Accepted 9th February 2026

DOI: 10.1039/d5ra05774d

[rsc.li/rsc-advances](http://rsc.li/rsc-advances)
<sup>a</sup>Center for Pharmaceutical Biotechnology, Duy Tan University, Da Nang 550000, Vietnam

<sup>b</sup>School of Pharmacy and Technology Management, SVKM's Narsee Monjee Institute of Management Studies (NMIMS), Deemed-to-be-University, Green Industrial Park, TSIIC, Jadcherla, Hyderabad 509301, India

<sup>c</sup>School of Pharmacy & Technology Management, SVKM's Narsee Monjee Institute of Management Studies (NMIMS) Deemed-to-University, Jadcherla - 509301, Hyderabad, India

<sup>d</sup>Department of Chemistry, Oklahoma State University, Stillwater 74078, Oklahoma, USA

<sup>e</sup>Pharmacology Department, AU College of Pharmaceutical Sciences, Andhra University, Visakhapatnam 530003, Andhra Pradesh, India

<sup>f</sup>Veterinary Medicine Teaching and Research Center, School of Veterinary Medicine, University of California, Davis, Tulare, CA, USA

<sup>g</sup>Department of Chemistry, Faculty of Science and Mathematics, Universiti Pendidikan Sultan Idris, Tanjong Malim, 35900, Perak, Malaysia

<sup>†</sup>Current address: Department of Neurology, O'Donnell Brain Institute, University of Texas Southwestern Medical Center, Dallas, TX 75390, USA.

## Introduction

Tuberculosis (TB) is a preventable and generally treatable contagious bacterial infection caused by *Mycobacterium tuberculosis* (*M.tb*), which spreads through the air when infected individuals expel the bacteria, for instance, through coughing.<sup>1,2</sup> In 2022, newly diagnosed TB cases reached 7.5 million globally, marking the highest figure since the WHO commenced global TB monitoring in 1995. In the same year, TB became the second leading cause of death after COVID-19 attributable to a single infectious agent worldwide, with a reported 1.3 million deaths, surpassing HIV/AIDS.<sup>3</sup> In 2023, 1.25 million TB-related deaths were reported.<sup>4</sup> Furthermore, the emergence of new cases involving multidrug-resistant (MDR) and extremely drug-resistant (XDR) TB strains that exhibit resistance to the first-line drugs, such as rifampicin<sup>5</sup> has resulted in significant global health challenges related to TB.<sup>6</sup> Globally, an estimated 400 000 people developed MDR/rifampicin-resistant TB<sup>4</sup>



emphasising the urgent need for the development of potent novel antimycobacterial agents with chemical structures capable of penetrating macrophages. These agents should impede the advancement of intracellular pathogens, addressing the pressing need to combat the threat posed by TB.

In the quest for novel antimycobacterial agents, we investigated the foliose lichen *Lobaria pulmonaria* (L.) Hoffm. (family: Lobariaceae), which has been used in ethnopharmacology for treating lung ailments such as TB, coughs, and haemoptysis since the late 1400s. *L. pulmonaria* was widely used throughout Europe until the 1600s.<sup>7–11</sup> For example, this lichen is referred to as “Oak Lung” or “Lungs of Oak” in English, “Lungenkraut” in German, “Toad Skin” in Chinese, “Crotal Coille” in Irish, “Muscus Pulmonarius” in Latin, and “Hazelraw” in Scottish cultures.<sup>12–15</sup> Typically, *L. pulmonaria* was prepared by boiling in water or milk or as a vegetable, using various cooking methods, including frying, making soup, steaming, stewing, and more for consumption.<sup>12–14</sup>

From a biological perspective, extracts of *L. pulmonaria* have been reported to have anti-inflammatory, antiulcerogenic, antioxidant, anti-proliferative, antimicrobial, apoptotic, and gastro-protective effects.<sup>16–22</sup> The chemical entities identified from extracts of *L. pulmonaria* include salazinic acid,<sup>23</sup> depsidone (C<sub>21</sub>H<sub>19</sub>O<sub>9</sub>),<sup>24</sup> gyrophoric acid, (±)atranorin, thelephoric acid, norstictic acid, constictic acid,<sup>25</sup> stictic acid,<sup>25–27</sup> rhizonaldehyde, isidiophorin, pulmonarianin, vesuvianic acid, rhizonyl alcohol, ergosterol-5 $\alpha$ ,8 $\alpha$ -peroxide,<sup>26</sup> and melanins.<sup>28</sup> However, their antimycobacterial activities remained to be elucidated.

*M.tb* possesses complex biosynthetic pathways involved in the synthesis of mycolic acids, peptidoglycan, and lipids, which contribute to its survival and virulence. Among these pathways, the fatty acid synthase (FAS) system is a key target for anti-*M.tb* compounds due to its role in building the lipid-rich cell wall that enables intracellular survival. The FAS system consists of two pathways: FAS-I, responsible for short-chain fatty acid synthesis, and FAS-II, which produces long-chain fatty acids. FabG, a ketoacyl reductase, is integral to FAS, with FabG1 and FabG4 being the only enzymes with conserved genes among mycobacterial species. FabG4, a high molecular weight NADH-dependent  $\beta$ -ketoacyl CoA reductase, catalyses the reduction of  $\beta$ -ketoacyl intermediates to  $\beta$ -hydroxyacyl derivatives, which is crucial for cell wall integrity and bacterial survival.<sup>29,30</sup> Additionally, FabG4 has been implicated in drug resistance, as it is overexpressed in response to sub-inhibitory concentrations of Streptomycin.<sup>30</sup>

Despite growing interest in natural products for TB treatment, there remains a notable gap in the evaluation of specific lichen-derived secondary metabolites against MDR-TB clinical isolates. While compounds such as calanolides have shown some antimycobacterial potential,<sup>31</sup> metabolites like fukinanolide A, pinastric acid, stictic acid, and scrobiculin have not been comprehensively studied in this context (to the best of our knowledge). This study addressed this gap by isolating these metabolites from the lichen *L. pulmonaria* and demonstrated their antimycobacterial efficacy against multiple MDR-TB strains. Additionally, we provide novel molecular docking evidence of these compounds, uncovering plausible mechanisms for their antimycobacterial action. Together, these findings substantiate the potential of these metabolites as

promising antimycobacterial agents and justify further investigation.

Thus, in the current study, we aimed to: (i) conduct bioassay-guided isolation process to extract antimycobacterial metabolites from *L. pulmonaria*; (ii) assess the antimycobacterial activity of the acetone extract of *L. pulmonaria* (LP) and its secondary metabolites against *M.tb* H37Ra and six other MDR-TB clinical isolates, (iii) evaluate the safety of LP extract and its secondary metabolites by measuring their cytotoxicity against human leukaemia monocytic (THP-1) macrophages, and (iv) uncover the mechanism of action of these compounds by docking them against key metabolic enzymes of *M.tb*, namely cytochrome P450 14 $\alpha$ -sterol demethylase (PDB ID: 1EA1), mycobacterial ATP synthase (PDB ID: 4V1F), and  $\beta$ -ketoacyl reductase FabG4 (PDB ID: 3V1U).

## Results and discussion

### Bioassay-guided isolation

The LP extract was subjected to an initial screening for antimycobacterial activity against *M.tb* H37Ra at six concentrations ranging from 0 to 100  $\mu\text{g mL}^{-1}$  using XRMA method (Table 1). The results confirmed its antimycobacterial activity with a half-maximal inhibitory concentration (IC<sub>50</sub>) value of  $7.74 \pm 0.27 \mu\text{g mL}^{-1}$  (Table 1 and Fig. 1). Subsequently, LP was subjected to fractionation through column chromatography (CC), resulting in six fractions (F1–6). The initial antimycobacterial assay of these compounds against *M.tb* H37Ra revealed the inhibition level of fractions F2, F3, and F5 exceeded 65%, while that of F1, F4, and F6 were below 27% at the concentration of 100  $\mu\text{g mL}^{-1}$  (Table 1). Among all fractions, F3 exhibited the highest antimycobacterial activity with an IC<sub>50</sub> value of  $6.26 \pm 0.04 \mu\text{g mL}^{-1}$ ; followed by F2 and F5, with IC<sub>50</sub> values of  $38.82 \pm 0.34$  and  $46.69 \pm 1.13 \mu\text{g mL}^{-1}$ , respectively (Table 1 and Fig. 1). Conversely, DMSO (2%) used for dilution did not show any *M.tb* H37Ra inhibitory activity.

Subsequently, the three fractions (F2, F3, and F5) with high antimycobacterial activity were subjected to further purification using CC, resulting in the isolation of four known metabolites that were later identified as fukinanolide A (F2), pinastric acid, stictic acid (F3), and scrobiculin (F5) (Fig. 1). This finding aligns with the outcomes of previous studies which identified stictic acid as a major chemical constituent in *L. pulmonaria*.<sup>25–27</sup> However, three other compounds identified in this study have not been previously isolated from *L. pulmonaria*; hence we report them for the first time.

All four secondary metabolites were similarly tested for antimycobacterial activity against *M.tb* H37Ra strain. Stictic acid demonstrated the highest inhibitory activity against *M.tb* H37Ra, comparable to that of LP extract (Table 1) with the IC<sub>50</sub> value of  $5.63 \pm 0.07 \mu\text{g mL}^{-1}$  ( $P < 0.0001$ ) (Table 1 and Fig. 1). Fukinanolide A showed moderate antimycobacterial activity with an IC<sub>50</sub> value of  $16.29 \pm 0.40 \mu\text{g mL}^{-1}$  ( $P < 0.0001$ ), while pinastric acid and scrobiculin exhibited significantly lower antimycobacterial activity with IC<sub>50</sub> values of  $31.31 \pm 1.06$  ( $P < 0.0001$ ) and  $24.34 \pm 0.47$  ( $P < 0.0001$ )  $\mu\text{g mL}^{-1}$ , respectively (Fig. 1 and Table 1). These results indicate that the observed



**Table 1** Yield obtained and screening of antimycobacterial actions of LP, F1–6, and isolated compounds from *Lobaria pulmonaria* (L.) Hoffm. against *M.tb* H37Ra using XRMA

Sample	Yield (mg)	Percentage inhibition of <i>M.tb</i> H37Ra <sup>a</sup>						IC <sub>50</sub> values <sup>a</sup> (μg mL <sup>-1</sup> )
		0 μg mL <sup>-1</sup>	5 μg mL <sup>-1</sup>	10 μg mL <sup>-1</sup>	25 μg mL <sup>-1</sup>	50 μg mL <sup>-1</sup>	100 μg mL <sup>-1</sup>	
LP	12 500	0.06 ± 0.01	33.57 ± 2.72	63.43 ± 1.56	73.46 ± 0.51	88.15 ± 1.42	95.37 ± 1.17	7.74 ± 0.27*
F1	950	0.04 ± 0.02	2.94 ± 0.15	4.23 ± 0.13	5.36 ± 0.04	9.21 ± 0.39	13.64 ± 1.16	>100
F2	550	0.03 ± 0.01	10.73 ± 0.43	22.43 ± 1.31	33.86 ± 1.99	63.07 ± 1.13	70.75 ± 0.95	38.82 ± 0.34*
F3	850	0.04 ± 0.01	41.81 ± 0.71	74.36 ± 1.13	89.79 ± 0.52	94.50 ± 0.37	98.37 ± 0.11	6.26 ± 0.04*
F4	900	0.03 ± 0.01	2.23 ± 0.18	3.82 ± 0.11	4.53 ± 0.18	8.73 ± 0.99	16.53 ± 0.33	>100
F5	600	0.03 ± 0.01	16.73 ± 1.06	29.31 ± 3.06	40.56 ± 2.59	51.74 ± 1.47	66.17 ± 3.19	46.69 ± 1.13*
F6	560	0.07 ± 0.02	1.59 ± 0.13	5.74 ± 0.35	7.70 ± 0.28	16.87 ± 1.00	27.46 ± 0.78	>100 <sup>b</sup>
Fukinanolide A	290	0.08 ± 0.15	22.00 ± 1.65	41.46 ± 0.79	61.81 ± 0.22	70.44 ± 2.15	78.12 ± 0.56	16.29 ± 0.40*
Pinastric acid	200	0.05 ± 0.02	19.46 ± 0.88	29.82 ± 0.23	46.33 ± 1.38	60.53 ± 1.67	70.45 ± 2.18	31.31 ± 1.06*
Stictic acid	250	0.10 ± 0.02	43.41 ± 0.85	71.75 ± 0.50	82.89 ± 1.85	91.94 ± 1.90	95.60 ± 1.34	5.63 ± 0.07*
Scrobiculin	350	0.08 ± 0.04	20.52 ± 1.38	27.92 ± 0.61	51.01 ± 0.72	66.20 ± 0.78	75.63 ± 0.66	24.34 ± 0.47*
Rifampicin	NA	0 μg mL <sup>-1</sup>	0.1 μg mL <sup>-1</sup>	0.2 μg mL <sup>-1</sup>	0.5 μg mL <sup>-1</sup>	1.0 μg mL <sup>-1</sup>	2.0 μg mL <sup>-1</sup>	0.149 ± 0.002
		0.09 ± 0.01	39.33 ± 0.56	61.13 ± 0.79	77.58 ± 1.07	88.43 ± 2.12	96.69 ± 0.87	

<sup>a</sup> Mean ± SD ( $n = 3$ ), <sup>b</sup> IC<sub>50</sub> values are expressed as μg mL<sup>-1</sup> (mean ± SD,  $n = 3$ ), where statistical analysis determined by Student's *t*-test, where \* $p < 0.0001$  were statistically significant compared to rifampicin. DMSO was used as a negative control.

antimycobacterial activity of the bioactive fractions of *L. pulmonaria* (F2, F3, and F5) may be attributed to these secondary metabolites.

### In vitro antimycobacterial activity

Based on the initial results, LP extract and all four isolated compounds were further evaluated for antimycobacterial activity at concentrations ranging from 0.244 to 500 μg mL<sup>-1</sup> to determine the minimum inhibitory concentration (MIC) against *M.tb* H37Ra and six MDR-TB strains (JAL-19049, JAL-

19126, JAL-19111, JAL-19187, JAL-19129, and JAL-19188) using the resazurin microtiter plate assay (REMA) method. Interestingly, all six tested MDR-TB strains exhibited higher susceptibility to LP (MICs ranged from 1.95 to 3.91 μg mL<sup>-1</sup>) compared to the *M.tb* H37Ra (MIC of 15.62 μg mL<sup>-1</sup>), indicating that LP was more potent in controlling the growth of all six tested MDR-TB isolates as compared to the drug-sensitive strain, *M.tb* H37Ra.

In addition, the REMA results demonstrated potent antimycobacterial activity of stictic acid and fukinanolide A against

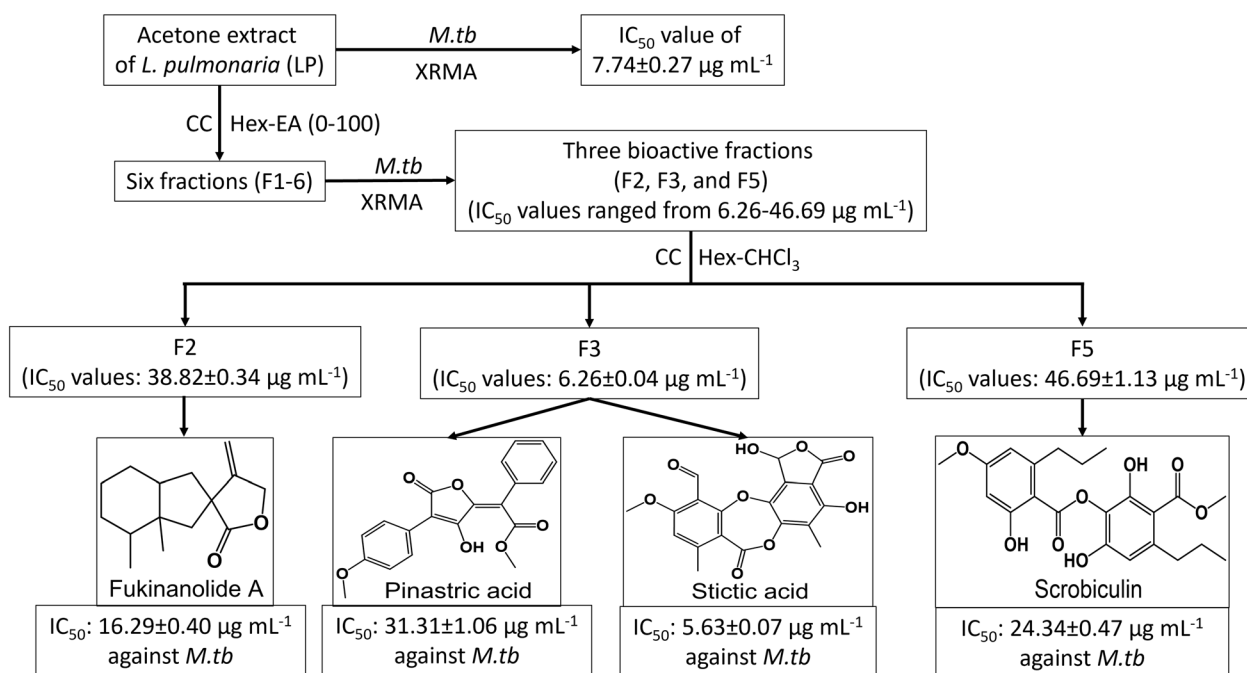


**Fig. 1** A flow chart of bioassay-guided isolation of secondary metabolites from acetone extract (LP) of *Lobaria pulmonaria* (L.) Hoffm. Values of half-maximal inhibitory concentrations (IC<sub>50</sub>) against *Mycobacterium tuberculosis* H37Ra (*M.tb*) were expressed as mean ± standard deviation ( $n = 3$ ). XRMA: 2,3-bis-(2-methoxy-4-nitro-5-sulfophenyl)-2H-tetrazolium-5-carboxanilide reduction menadione assay; CC: column chromatography; Hex: *n*-hexane; EA: ethyl acetate; CHCl<sub>3</sub>: chloroform.



Table 2 Antimycobacterial activity, cytotoxicity, and selectivity index of LP extract and isolated compounds from *Lobaria pulmonaria* (L.) Hoffm.

Sample	Cytotoxicity <sup>a</sup>	<i>M.tb</i> H37Ra		JAL-19049		JAL-19111		JAL-19126		JAL-19129		JAL-19187		JAL-19188	
		MIC <sup>b</sup>	SI	MIC <sup>b</sup>	SI	MIC <sup>b</sup>	SI	MIC <sup>b</sup>	SI	MIC <sup>b</sup>	SI	MIC <sup>b</sup>	SI	MIC <sup>b</sup>	SI
LP	169.53 ± 1.22*	15.62	11	1.95	87	3.91	43	3.91	43	1.95	87	1.95	87	1.95	87
Fukinanolide A	146.05 ± 0.93*	31.25	5	15.62	9	31.25	5	31.25	5	7.81	19	31.25	5	31.25	5
Pinastric acid	193.18 ± 1.34*	62.50	3	62.50	3	250.00	1	125.00	2	62.50	3	62.50	3	250.00	1
Stictic acid	104.47 ± 3.38*	3.91	27	3.91	27	7.81	13	7.81	13	1.95	54	1.95	54	7.81	13
Scrobiculin	170.91 ± 1.82*	62.50	3	250.00	1	31.25	5	62.50	3	31.25	5	125.00	1	500.00	0
Rifampicin	106.20 ± 1.08*	0.20	531	100.00	1	50.00	2	12.50	8	25.00	4	50.00	2	100.00	1
Doxorubicin	8.46 ± 0.32	NT	NT	NT	NT	NT	NT	NT	NT	NT	NT	NT	NT	NT	NT

<sup>a</sup> IC<sub>50</sub> values are expressed as  $\mu\text{g mL}^{-1}$  (mean  $\pm$  SD,  $n = 3$ ), where statistical analysis determined by Student's *t*-test, where \* $p < 0.0001$  was statistically significant compared to standard drug. <sup>b</sup> MIC are expressed as  $\mu\text{g mL}^{-1}$  ( $n = 3$ ), where SD values are 0.00 for all samples, indicating no variation among replicates; thus, differences between test groups and rifampicin are considered highly significant ( $p < 0.0001$ ). DMSO was used as a negative control.

both *M.tb* and six MDR-TB isolates, with MICs ranging from 1.95 to 31.25  $\mu\text{g mL}^{-1}$  (Table 2). In comparison, the standard rifampicin showed potent antimycobacterial activity against *M.tb* (MIC of 0.2  $\mu\text{g mL}^{-1}$ ), but had significantly lower activity against the tested MDR-TB strains (MICs ranging from 12.50 to 100.00  $\mu\text{g mL}^{-1}$ ), potentially attributable to resistance exhibited by these clinical isolates to first-line anti-TB drugs.<sup>32</sup>

Among the bioactive metabolites, stictic acid demonstrated remarkable inhibitory activity against all six MDR-TB isolates, with MICs ranging from 1.95 to 7.81  $\mu\text{g mL}^{-1}$ , surpassing rifampicin (MIC: 12.5–100  $\mu\text{g mL}^{-1}$ ) (Table 2). However, the other metabolites exhibited selective antimycobacterial activity against the different MDR-T strains; fukinanolide showed enhanced inhibitory activity against JAL-19049 (MIC: 15.62  $\mu\text{g mL}^{-1}$ ) and JAL-19129 (MIC: 7.81  $\mu\text{g mL}^{-1}$ ), scrobiculin was active against JAL-19111 and JAL-19129 (MIC: 31.25  $\mu\text{g mL}^{-1}$ ), and pinastric acid was active against JAL-19049 (MIC: 62.50  $\mu\text{g mL}^{-1}$ ) only (Table 2). In contrast, DMSO (2%) used for dilution (two-fold) showed no inhibition against all tested mycobacterial strains. These findings demonstrated that stictic acid and fukinanolide A were remarkably potent in controlling the growth of the tested MDR-TB isolates as compared to rifampicin.

While pinastric acid and scrobiculin demonstrated selective antimycobacterial activity primarily against MDR-TB isolates, they showed relatively higher MICs or lower SI against the standard *M.tb* H37Ra strain. This selective efficacy may reflect distinct mechanisms of action or target specificity that are more effective against resistant strains, possibly through interactions with resistance-related pathways or altered metabolic states in MDR bacteria. These findings suggest potential for these compounds to be developed as adjunct or alternative therapies specifically targeting MDR-TB infections.

Compared to its isolated compounds and rifampicin, the LP extract exhibited superior antimycobacterial activity against six tested MDR-TB isolates. This superior activity of the LP extract could be attributable to the synergistic effect of its chemical constituents. This phenomenon has been observed previously, in which combining a natural secondary metabolite 7-methyljuglone, with rifampicin resulted in a 4-fold reduction in the MIC and demonstrated synergistic activity against both

intracellular and extracellular *M.tb*.<sup>33</sup> Moreover, stictic acid, fukinanolide A, and scrobiculin showed increased inhibition of MDR-TB strains with significantly lower MICs than rifampicin, suggesting these secondary metabolites are the key bioactive compounds present in the folkloric lichen *L. pulmonaria*.

#### Cytotoxicity assay

Since the alveolar macrophages are the initial target of *M.tb* during the early phase of infection, the LP extract and its isolated secondary metabolites were tested for cytotoxicity to THP-1 macrophages using the MTT assay. The results revealed that the IC<sub>50</sub> values of LP extract (169.53  $\pm$  1.22  $\mu\text{g mL}^{-1}$ ), stictic acid (104.47  $\pm$  3.38  $\mu\text{g mL}^{-1}$ ) and fukinanolide A (146.05  $\pm$  0.93  $\mu\text{g mL}^{-1}$ ) on THP-1 macrophages were considerably higher than their MICs against *M.tb* and six tested MDR-TB isolates (Table 2). Furthermore, these IC<sub>50</sub> values were considerably higher ( $P < 0.0001$ ) than that of the reference compound doxorubicin (IC<sub>50</sub>: 8.46  $\pm$  0.32  $\mu\text{g mL}^{-1}$ ) (Table 2). This observation suggests that THP-1 macrophages were not adversely impacted at concentrations effective against *M.tb* and six tested MDR-TB isolates and that stictic acid and fukinanolide A are biocompatible.

#### Selectivity index

Additionally, the selectivity index (SI, IC<sub>50</sub>/MIC) for LP extract, stictic acid, and fukinanolide A was assessed to gauge the safety and effectiveness as drugs.<sup>34</sup> High SI values indicate lower toxicity and greater bioactivity of a compound. Our results showed that the SI ratio values of LP extract (SI: 11–87), stictic acid (SI: 13–54), and fukinanolide A (SI: 5–19) against six MDR-TB isolates were higher than those of the reference drug rifampicin (SI: 1–8) (Table 2). These results suggested that LP, stictic acid, and fukinanolide A are safe and potent against the six tested MDR-TB isolates compared to *M.tb*.

#### Molecular docking studies

To shed light on the possible molecular interactions and mechanisms of action of these compounds against *M.tb*, all four isolated secondary metabolites of *L. pulmonaria* were docked onto three crucial *M.tb* enzymes, namely cytochrome P450 14 $\alpha$ -sterol demethylase, mycobacterial ATP synthase, and  $\beta$ -ketoacyl reductase.





**Table 3** Binding energy,  $K_i$  values and interactions of fukinanolide A, pinastic acid, stictic acid, and scrobiculin against cytochrome P450 14 $\alpha$ -sterol demethylase (PDB ID: 1EA1), mycobacterial ATP synthase (PDB ID: 4V1F),  $\beta$ -ketoacyl reductase FabG4 (PDB ID: 3V1U) and compared with their internal pre-docked ligands

Compound	Demethylase (1EA1)		ATP synthase (4V1F)		$\beta$ -Ketoacyl reductase (3V1U)		Interaction (H-bond and $\pi$ - $\pi$ )
	kcal mol <sup>-1</sup>	$K_i$	kcal mol <sup>-1</sup>	$K_i$	kcal mol <sup>-1</sup>	$K_i$	
Fukinanolide A	-9.3	151.80 nM	-5.01	214.34 $\mu$ M	-6.53	16.28 $\mu$ M	—
Pinastic acid	-8.95	274.59 nM	-4.56	455.61 $\mu$ M	-6.93	8.27 $\mu$ M	Glu65 (1.83 Å)
Stictic acid	-7.2	5.28 $\mu$ M	-5.25	141.64 $\mu$ M	-6.53	16.48 $\mu$ M	Glu65 (1.73 Å)
Scrobiculin	-9.13	203.27 nM	-2.53	13.98 mM	-5.36	117.94 $\mu$ M	Gly62 (2.24 Å)
Internal ligand	-7.67	2.37 $\mu$ M	-6.2	10.46 $\mu$ M	-3.73	1.84 mM	—
							Ser347 (1.70 Å) Phe392 (1.61 Å) Ser347 (2.1 Å), Gln357 (2.08 Å) Ala349 (1.89 Å) Asn354, Arg355, Gln357

The binding energies and inhibition constants of all the molecules have been calculated and presented in Table 3. It was observed that all four molecules bind to the active site of cytochrome P450 14 $\alpha$ -sterol demethylase, specifically channel 2 located near the N terminal of this protein (Fig. 3, highlighted in blue). These molecules formed hydrogen bonds and  $\pi$ - $\pi$  interactions with different amino acid residues like Arg96, His259, and Hem460, and completely occupied the channel 2 or the substrate binding site of the protein (Fig. 3A–E) with high binding affinities ranging from  $-7.2$  to  $-9.3$  kcal mol<sup>-1</sup>. This interaction induces conformational changes around residues 253–255 and closes the BC loop,<sup>35</sup> thereby inhibiting the enzyme activity.

The internal ligand, on the other hand, formed a hydrogen bond with Arg96 (Fig. 3F), but because it sits slightly away from the  $\beta$ 1–4 loop, mostly due to its binding orientation, its binding energy with the target protein was lower ( $-7.67$  kcal mol<sup>-1</sup>) compared to all of the isolated molecules, except for stictic acid ( $-7.2$  kcal mol<sup>-1</sup>). Similarly, these molecules were docked against mycobacterial ATP synthase, another vital enzyme for the growth of *M.tb*.<sup>36</sup> In general, binding of an inhibitor to ion-binding region (Fig. 4C, highlighted in yellow) will block other ions from binding and thus inhibit the ATP synthesis reaction.<sup>37</sup> Our docking results showed that all four molecules and the internal ligand interact with this protein in a similar manner and validates the docking protocol (Fig. 2C). Specifically, these molecules bind to the F<sub>o</sub> domain of the ion-binding region and completely occupied the hydrophobic pocket by forming hydrogen bonds with different amino acid residues like Gly62 or Glu65 (Fig. 4A–F). These interactions prevent the C-ring rotation and thus inhibit the ion exchange in F<sub>o</sub> domain, thereby completely blocking ATP synthase.<sup>37–39</sup>

Lastly, we docked all the compounds against  $\beta$ -oxoacyl reductase, another crucial enzyme in *M.tb* involved in fatty acids synthesis.<sup>40</sup>  $\beta$ -oxoacyl reductase has a major groove, that interacts with NADPH and a minor groove that binds to the hexanoyl-CoA to form an enzyme–NADPH–CoA ternary complex to elongate the fatty-acyl chain.<sup>40,41</sup> Asn319, Ser347, Tyr360, and Arg 445 form the active site pocket, located in the minor groove near the C-terminal (Fig. 5A, highlighted in yellow).<sup>30</sup> Inhibitors often compete with hexanoyl-CoA for binding to the minor groove of this enzyme. The docking results showed that the four molecules formed hydrogen bonds with Ser347, Ala349, Gln357, and Phe392 (Fig. 5B–E), while the internal ligand, hexanoyl-CoA, formed hydrogen bonds with Asn354, Arg355, Gln357, and Thr405 residues (Fig. 5F).

The results showed that, our molecules bind to the enzyme with higher binding energy (ranging from  $-5.36$  to  $-6.93$  kcal mol<sup>-1</sup>) compared to the internal ligand ( $-3.73$  kcal mol<sup>-1</sup>). Notably, our molecules bind and completely occupy the catalytic binding site of the enzyme and would therefore stop fatty acid chain elongation. Overall, the results of our molecular docking study showed that all four molecules bind to cytochrome P450 14 $\alpha$ -sterol demethylase and  $\beta$ -ketoacyl reductase with high affinity. Specifically, all four molecules bind to  $\beta$ -ketoacyl reductase with a significantly higher affinity compared to its internal ligand (Table 3). Therefore, the docking results indicated specific binding of the isolated molecules to

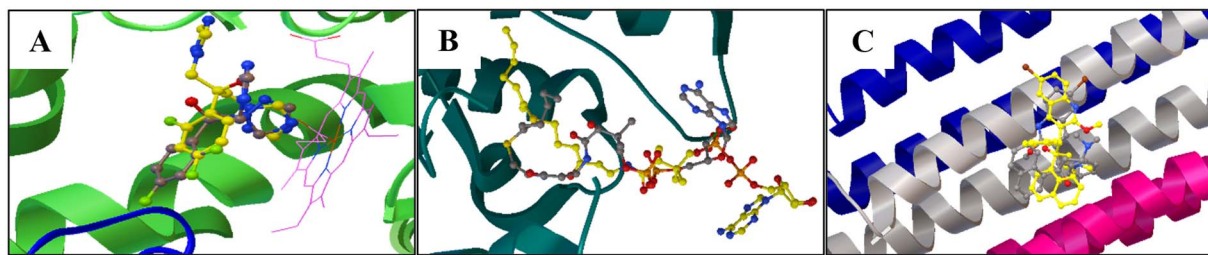


Fig. 2 Superimposing of co-crystal ligand (yellow) and redocking of co-crystal ligand (grey) for docking validation. (A) Cytochrome P450 14 $\alpha$ -sterol demethylase (PDB ID: 1EA1) with RSM of 2.5 Å; (B)  $\beta$ -ketoacyl reductase FabG4 (PDB ID: 3V1U) with RSM of 4.53 Å; (C) mycobacterial ATP synthase rotor ring (PDB ID: 4V1F) with RSM of 2.83 Å.

key enzymes, including cytochrome P450 14 $\alpha$ -sterol demethylase and  $\beta$ -ketoacyl reductase, resulting in the inactivation of these enzymes and imparting strong antimycobacterial activity to the isolated molecules.

Overall, our findings that fukinanolide A and stictic acid effectively inhibit the growth of several MDR-TB isolates

represent a significant advancement over existing literature, which lacks detailed antimycobacterial evaluation of these metabolites. Previous studies had primarily reported antimicrobial activity of lichen metabolites in general,<sup>42</sup> with limited focus on drug-resistant *M.tb*. The superior efficacy of these compounds compared to rifampicin in our assays highlights

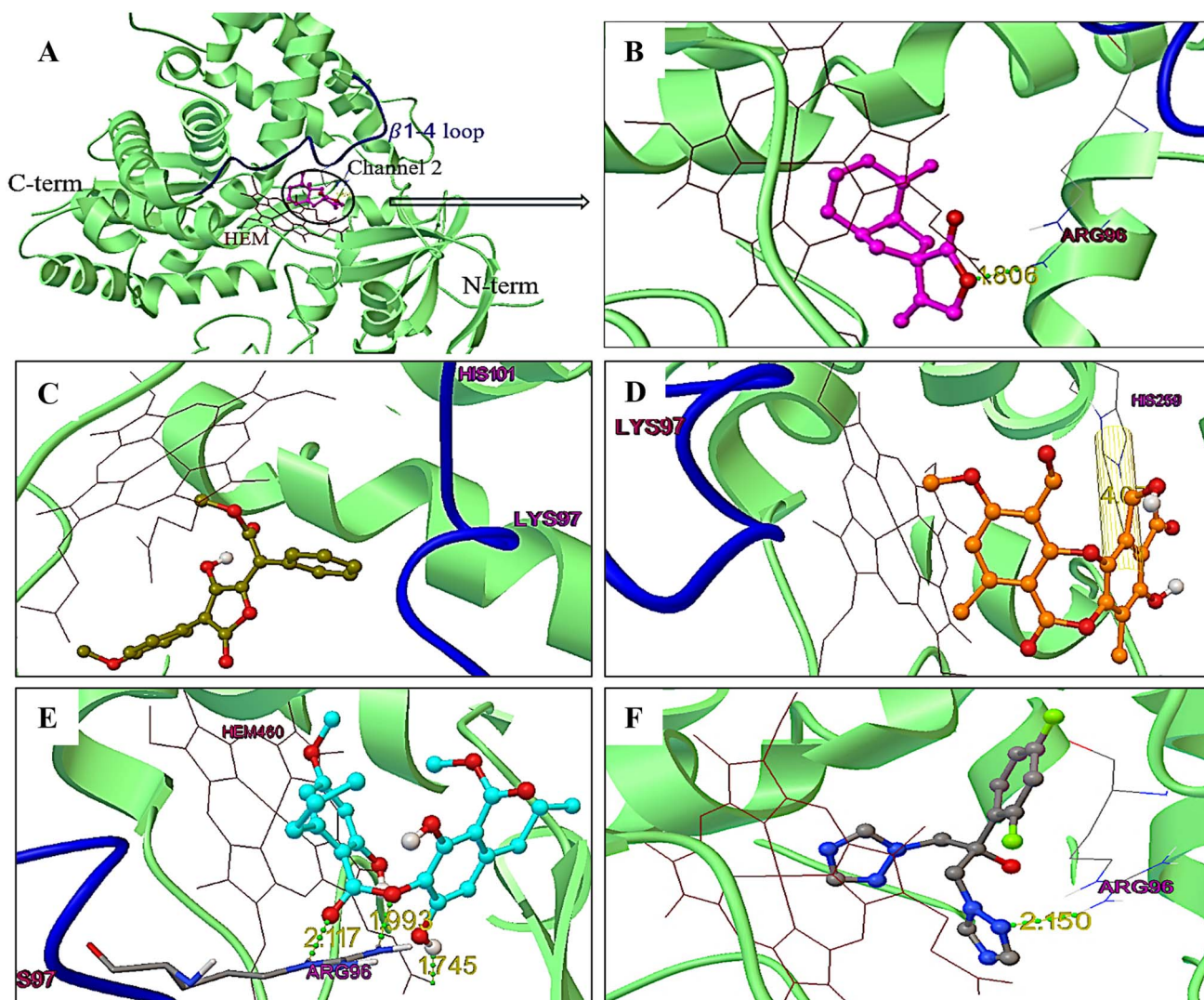


Fig. 3 Binding interaction of (A) and (B) fukinanolide A; (C) pinastric acid; (D) stictic acid; (E) scrobiculin and (F) internal ligand in the active site of cytochrome P450 14 $\alpha$ -sterol demethylase (PDB ID: 1EA1).  $\beta$ 1–4 loop is shown in blue colour, HEM is shown in brown colour, and the rest of the protein is shown in green.



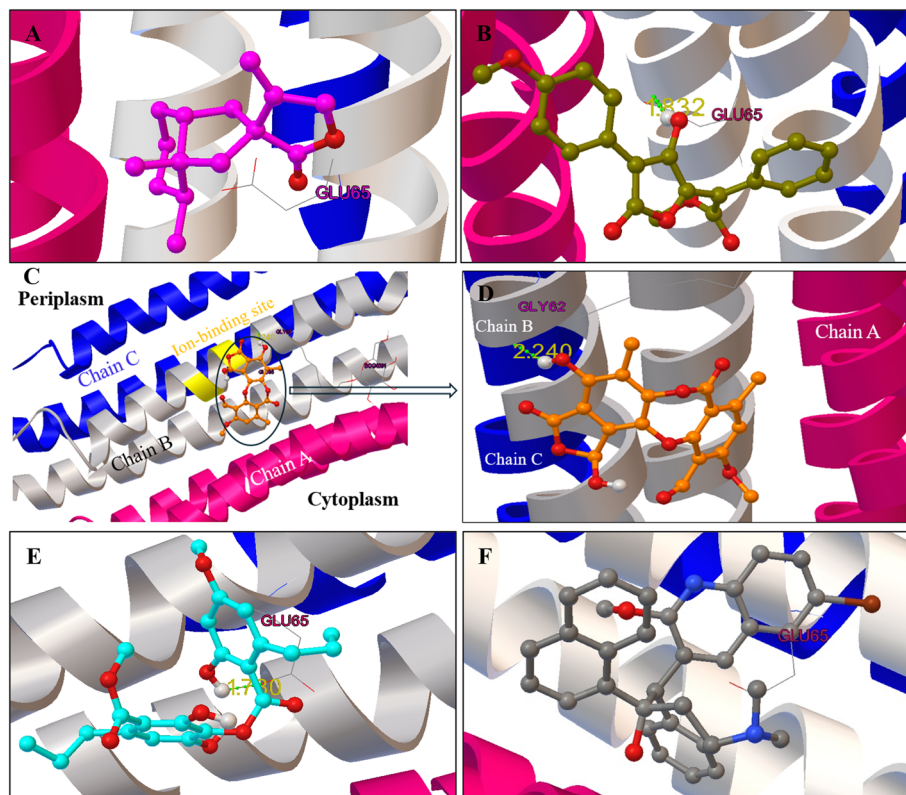


Fig. 4 Binding interaction of (A) fukinanolide A; (B) pinacric acid; (C) and (D) stictic acid; (E) scrobiculin and (F) internal ligand in the active site of mycobacterial ATP synthase rotor ring (PDB ID: 4V1F). Chain A, B and C have been shown in cyan, grey and blue colour respectively.

their therapeutic potential. Furthermore, the molecular docking studies corroborate a novel mechanism by demonstrating selective and potent binding to the FabG4 enzyme, a target scarcely explored in the context of these metabolites. These integrated bioactivities and *in silico* insights collectively underscore the relevance of lichen-derived secondary metabolites in combating MDR-TB.

Hence, to advance the promising *in vitro* findings of this study toward clinical application, future work should focus on *in vivo* validation using relevant animal model. These studies will be useful to assess pharmacokinetics, bioavailability, therapeutic efficacy, and safety profiles of *L. pulmonaria* extracts and isolated metabolites in a complex biological context. Additional research might explore formulation optimization to improve delivery and potency, as well as combinational studies with existing anti-TB drugs to evaluate synergistic effects. Toxicological studies and dose optimization will be essential prerequisites for progressing these compounds toward clinical trials. Together, these investigations will help bridge the gap between traditional ethnopharmacological knowledge and modern anti-MDR-TB drug development.

## Experimental

### Collection of lichen material

In January 2022, lichen *Lobaria pulmonaria* (L.) Hoffm. was gathered from plants on Son Tra Mountain in Da Nang, Vietnam (16.0609°N and 108.1248°E), situated at an elevation of 692

m above sea level. A voucher specimen (22–1038) was duly collected and deposited at the CSIR-National Botanical Research Institute in Lucknow, India.

### Extraction and bioassay-guided isolation

Approximately 150 g of dried *L. pulmonaria* was coarsely ground and subjected to the acetone extraction process three times in 250 mL volume at room temperature. The resulting combined extracts were evaporated using a rotavapor (Shimadzu Rotation Evaporator QR 2005-S, Japan), yielding LP in the form of a brown solid with a total yield of 12.5 g. The initial assessment of the LP extract for antimycobacterial activity was conducted against the *M.tb* H37Ra strain, following the protocol established earlier by our group.<sup>43</sup>

Approximately 10.0 g of LP was fractionated by chromatography using a sintered disc column (Borosil, India) packed with silica gel (230–400 mesh size, Merck, India), and utilising a *n*-hexane–ethyl acetate gradient (0–100%). Subsequently, all fractions were evaluated for antimycobacterial activity against the *M.tb* strain as described.<sup>43</sup> The fractions that exhibited inhibitory activity were subjected to additional purification to isolate bioactive secondary metabolites.

F2 (550 mg), F3 (850 mg), and F5 (600 mg) underwent successive CC using a sintered disc column (Borosil, India) with a *n*-hexane–chloroform gradient (0–100%) for isolation of secondary metabolites. All isolated compounds were analysed by Nuclear Magnetic Resonance (NMR) (Bruker Avance 400



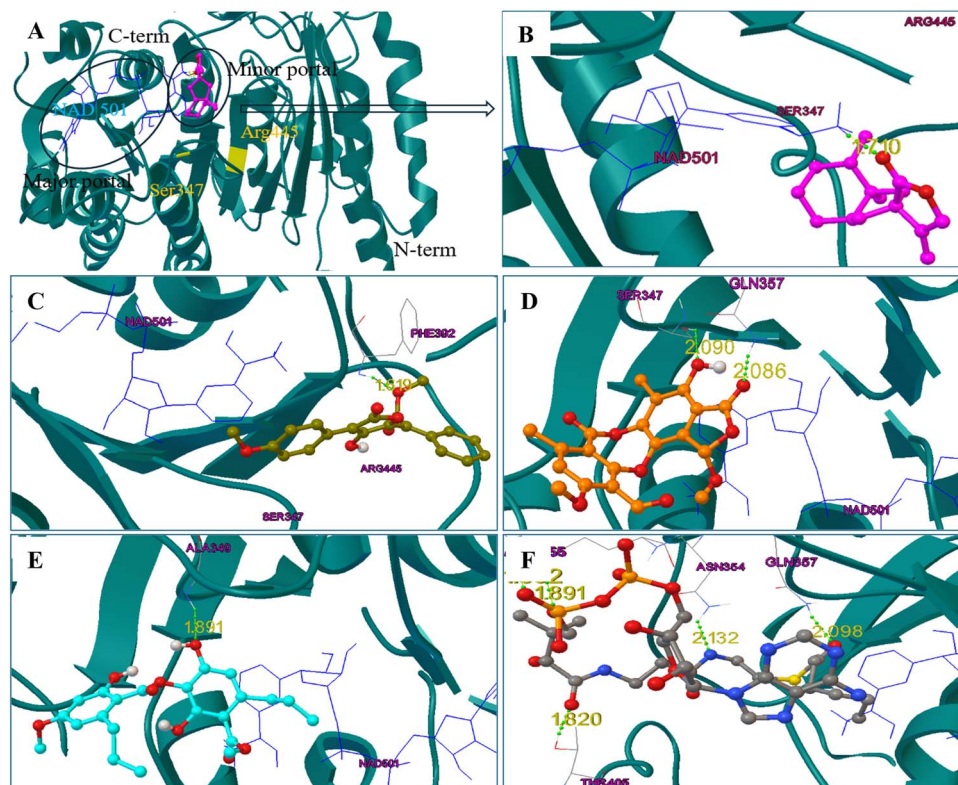


Fig. 5 Binding interaction of (A) and (B) fukinanolide A; (C) pinastric acid; (D) stictic acid; (E) scrobiculin and (F) internal ligand in the active site of  $\beta$ -ketoacyl reductase FabG4 (PDB ID: 3V1U), shown in dark cyan colour.

Spectrometer, Germany) and mass spectrometry (LC/MS Triple Quad Portfolio, Agilent, China) using Bruker's topspin software and Robust mass spectrometry software, respectively, to characterise the chemical properties (Table 4).

**Fukinanolide A.** M.p.: 80–81 °C;  $R_f$ : 0.4 (Hex-CHCl<sub>3</sub>, 9 : 1).  $[\alpha]_D^{25}$ : +17.1 (methanol). <sup>1</sup>H NMR (400 MHz, CDCl<sub>3</sub>): 0.98 (s, 3H, 15-CH<sub>3</sub>), 1.00 (s, 3H, 14-CH<sub>3</sub>), 1.12–1.16 (m, 2H, 3,5-CH), 1.26–1.36 (m, 2H, 2-CH), 1.52–1.70 (m, 5H, 1,6,7a-CH), 1.76–1.79 (m, 1H, 9a-CH), 1.86–1.88 (m, 1H, 7b-CH), 1.91–1.95 (m, 1H, 9b-CH), 4.70 (s, 2H, 11-CH), 5.11 (s, 2H, 13-CH) (Fig. S1).<sup>44</sup> <sup>13</sup>C NMR (400 MHz, CDCl<sub>3</sub>): 15.83 (C-14), 16.12 (C-15), 23.89 (C-1), 28.82 (C-6), 30.44 (C-2), 37.23 (C-7), 38.61 (C-3), 39.23 (C-9), 43.62 (C-4), 43.98 (C-5), 56.11 (C-8), 73.12 (C-11), 106.51 (C-13), 140.30 (C-12), 182.93 (C-10) (Fig. S2).<sup>44</sup> CHNS analysis for C<sub>15</sub>H<sub>22</sub>O<sub>2</sub>: calcd C-76.88%, H-9.46%, found C-76.86%, H-9.46%. ESI-MS calcd  $m/z$  for C<sub>15</sub>H<sub>22</sub>O<sub>2</sub>: 234.16 [M], found: 235.21 [M + H<sup>+</sup>] (Fig. S3).

**Pinastric acid.** M.p.: 202–203 °C;  $R_f$ : 0.6 (Hex-CHCl<sub>3</sub>, 3 : 2). <sup>1</sup>H NMR (400 MHz, CDCl<sub>3</sub>): 3.12 (s, 1H, 8-OH, D<sub>2</sub>O-exchangeable), 3.81 (s, 3H, 20-OCH<sub>3</sub>), 3.87 (s, 3H, 13-OCH<sub>3</sub>), 6.83–6.84 (d, 2H,  $J = 4$  Hz, 3,5-Ar-H), 7.16–7.27 (m, 7H, 2,6,15,16,17,18,19-Ar-H) (Fig. S4A and B).<sup>44</sup> <sup>13</sup>C NMR (CDCl<sub>3</sub>, 400 MHz):  $\delta$  51.71 (C-13), 55.72 (C-20), 98.56 (C-7), 113.71 (C-11), 114.64 (C-3/5), 121.01 (C-1), 128.88 (C-16/18), 129.44 (C-2/6), 130.12 (C-15/19), 130.31 (C-14), 130.75 (C-17), 154.81 (C-9), 158.26 (C-4), 163.46 (C-8), 169.24 (C-12), 169.67 (C-10) (Fig. S5).<sup>44</sup> CHNS analysis for C<sub>20</sub>H<sub>16</sub>O<sub>6</sub>: calcd C-68.18%, H-

4.58%, found C-68.76%, H-4.54%. ESI-MS calcd  $m/z$  for C<sub>20</sub>H<sub>16</sub>O<sub>6</sub>: 352.09 [M], found: 351.15 [M – H<sup>+</sup>] (Fig. S6).

**Stictic acid.** M.p.: 271–272 °C;  $R_f$ : 0.4 (Hex-CHCl<sub>3</sub>, 3 : 2). <sup>1</sup>H NMR (DMSO-*d*<sub>6</sub>, 400 MHz): 1.72 (s, 1H, 15-OH, D<sub>2</sub>O-exchangeable), 2.32 (s, 3H, 19-CH<sub>3</sub>), 2.37 (s, 3H, 18-CH<sub>3</sub>), 3.25 (s, 2H, 11, 15-OH, D<sub>2</sub>O-exchangeable), 3.85 (s, 3H, 17-OCH<sub>3</sub>), 6.79 (s, 1H, 8-Ar-H), 8.20 (s, 1H, 16-CHO) (Fig. S7A and B).<sup>44</sup> <sup>13</sup>C NMR (DMSO-*d*<sub>6</sub>, 400 MHz):  $\delta$  8.32 (C-19), 21.51 (C-18), 57.57 (C-17), 96.89 (C-15), 110.68 (C-12), 114.28 (C-8), 114.38 (C-2), 117.84 (C-6), 125.03 (C-10), 134.37 (C-13), 139.89 (C-5), 149.42 (C-9), 149.86 (C-4), 155.89 (C-11), 160.32 (C-7), 162.46 (C-3), 165.38 (C-1), 167.02 (C-14), 186.09 (C-16) (Fig. S8).<sup>44</sup> CHNS analysis for C<sub>19</sub>H<sub>14</sub>O<sub>9</sub>: calcd C-59.07%, H-3.65%, found C-59.04%, H-3.63%. ESI-MS calcd  $m/z$  for C<sub>19</sub>H<sub>14</sub>O<sub>9</sub>: 386.06 [M], found: 385.80 [M – H<sup>+</sup>] (Fig. S9).

**Scrobiculin.** M.p.: 135–136 °C;  $R_f$ : 0.4 (Hex-CHCl<sub>3</sub>, 1 : 1). <sup>1</sup>H NMR (400 MHz, DMSO-*d*<sub>6</sub>): 0.88–0.97 (m, 6H, 9,9'-CH<sub>3</sub>), 1.59–1.65 (dd, 4H, 8, 8'-CH<sub>2</sub>), 2.51 (t, 1H,  $J = 4$  Hz, 2-OH, D<sub>2</sub>O-exchangeable), 2.82–2.87 (m, 4H, 7,7'-CH<sub>2</sub>), 3.78 (s, 3H, 10-OCH<sub>3</sub>), 3.84 (s, 3H, 10'-OCH<sub>3</sub>), 6.39–6.41 (dd, 2H,  $J = 4$  Hz, 3,5-Ar-H), 6.61 (s, 1H, 16-Ar-H), 10.50 (s, 1H, 17-OH, D<sub>2</sub>O-exchangeable), 11.85 (s, 1H, 13-OH, D<sub>2</sub>O-exchangeable) (Fig. S10A and B).<sup>44</sup> <sup>13</sup>C NMR (400 MHz, DMSO-*d*<sub>6</sub>): 14.50 (C-9), 14.60 (C-9'), 24.87 (C-8), 25.21 (C-8'), 36.88 (C-7), 37.82 (C-7'), 55.75 (C-10), 56.53 (C-10'), 99.46 (C-3), 106.21 (C-1), 108.59 (C-16), 108.80 (C-14), 109.51 (C-5), 125.19 (C-12), 144.12 (C-15), 145.96 (C-6), 154.34 (C-13), 154.73 (C-17), 160.63 (C-2), 162.92 (C-4), 166.74 (C-11), 172.65 (C-18) (Fig. S11).<sup>44</sup> CHNS analysis for



Table 4 Summary of physicochemical properties and biological activities of isolated lichen compounds

Compound (mol. form.)	R <sub>f</sub> value	M.p. (°C)	Spectral highlights	Antimycobacterial activity
Fukinanolide A (C <sub>15</sub> H <sub>22</sub> O <sub>2</sub> )	0.4 (Hex-CHCl <sub>3</sub> , 9 : 1)	80–81	- δ 0.98 and 1.00 ppm assignable to two methyl groups at positions 15 and 14, respectively - δ 182.93 ppm indicative of a carbonyl carbon at position 10	- Exhibited potent antimycobacterial activity with MICs ranging from 7.81 to 31.25 µg mL <sup>-1</sup> against MDR <i>M.tb</i> isolates - Showed moderate cytotoxicity and SI up to 19
Pinastric acid (C <sub>20</sub> H <sub>16</sub> O <sub>6</sub> )	0.6 (Hex-CHCl <sub>3</sub> , 3 : 2)	202–203	- Methoxy singlets at δ 3.81 and 3.87 ppm corresponding to positions 20 and 13, respectively - Deshielded aromatic carbons at δ 154.81 and 158.26 ppm characteristic of oxygenated aromatic carbons (C-9, C-4)	- Displayed relatively weak antimycobacterial activity with MICs up to 250 µg mL <sup>-1</sup> against MDR strains - Showed low cytotoxicity and low SI (1–3)
Stictic acid (C <sub>19</sub> H <sub>14</sub> O <sub>9</sub> )	0.4 (Hex-CHCl <sub>3</sub> , 3 : 2)	271–272	- Singlet at δ 3.85 ppm for a methoxy group (17-OCH <sub>3</sub> ) and aldehyde proton at δ 8.20 ppm (16-CHO) - δ 186.09 ppm indicative of a carbonyl carbon at position 16	- Demonstrated potent antimycobacterial effect with MICs as low as 1.95–7.81 µg mL <sup>-1</sup> against MDR strains - Exhibited moderate cytotoxicity with high SI up to 54
Scrobiculin (C <sub>22</sub> H <sub>26</sub> O <sub>8</sub> )	0.4 (Hex-CHCl <sub>3</sub> , 1 : 1)	135–136	- Downfield hydroxyl proton singlets at δ 10.50 and 11.85 ppm (17-OH, 13-OH) - δ 172.65 and 166.74 ppm corresponding to carboxyl or ester carbonyl carbons (C-18, C-11)	- Showed weak to moderate antimycobacterial activity with MICs from 31.25 to 500.00 µg mL <sup>-1</sup> against different MDR strains - Displayed moderate cytotoxicity and low SI for some strains

C<sub>22</sub>H<sub>26</sub>O<sub>8</sub>: calcd C-63.15%, H-6.26%, found C-63.11%, H-6.24(%). ESI-MS calcd *m/z* for C<sub>22</sub>H<sub>26</sub>O<sub>8</sub>: 418.16 [M], found: 417.00 [M – H<sup>+</sup>] (Fig. S12).

### In vitro antimycobacterial activity

The non-virulent *M.tb* strain (ATCC 25177) and six characterised MDR-TB isolates (JAL-19049, JAL-19126, JAL-19111, JAL-19187, JAL-19129, and JAL-19188), which demonstrated resistance to first-line anti-TB drugs (rifampicin, ethambutol, and isoniazid),<sup>32,45</sup> were acquired from the National JALMA Institute for Leprosy and Other Mycobacterial Diseases repository in Agra, India.

A suspension of the mycobacterial strain was prepared by resuspending *M.tb* colonies using 2 µL loops in 3 mL of Middlebrook 7H9 medium (Merck, India), contained in 5 mL sterile glass vials equipped with glass beads. The mixture was homogenised using a shaker. Subsequently, the McFarland turbidity of the suspension was adjusted to 1.0 and further diluted to a ratio of 1 : 20 in 7H9 medium.

The initial screening for antimycobacterial activity of LP, F1–6, and isolated metabolites against *M.tb strain* was conducted at 0, 5, 10, 25, 50, and 100 µg mL<sup>-1</sup> concentrations using 2%

DMSO in triplicate and employed the XRMA at 470 nm as described earlier.<sup>43</sup> In brief, in a 96-well plate, 250 µL of the previously prepared *M.tb* culture was combined with the test sample and 2,3-bis-(2-methoxy-4-nitro-5-sulfophenyl)-2H-tetrazolium-5-carboxanilide (XTT) (200 µM). The mixture was then incubated at 37 °C for 20 min. Subsequently, a Spectramax plate reader (at 470 nm) was used to measure the optical density of the tested samples from which the percentage inhibition and IC<sub>50</sub> values of *M.tb* was deliberated.

The antimycobacterial activity of the LP, isolated secondary metabolites, and the reference drug, rifampicin, was evaluated at concentrations ranging from 0.24 to 500 µg mL<sup>-1</sup> and 0.10 to 200 µg mL<sup>-1</sup>, respectively, against *M.tb* and six other MDR-TB strains, while 2% DMSO was used as a negative control. The tests were performed in triplicate using the REMA.<sup>43</sup> Specifically, in a 96-well plate, 100 µL of the previously prepared *M.tb*-MDR culture was combined with the test sample and XTT (200 µM). The mixture was then incubated at 37 °C for 7 days. Subsequently, 30 µL of 0.02% resazurin solution was added to each well and incubated for an additional 48 h. The MICs were then determined based on the observed colour change from blue to pink using a Spectramax pro5 plate reader (Molecular Devices Inc.).



### Cytotoxicity assay

The cytotoxicity of the LP and isolated compounds was assessed using the MTT assay<sup>46</sup> against human THP-1 macrophages. THP-1 monocytes were obtained from the National Centre for Cell Science (Pune, India), and maintained in RPMI-1640 medium (Merck, India), at 37 °C and 5% CO<sub>2</sub>. THP-1 monocytes were differentiated into macrophages one day prior to the infection experiment in a 96-well plate at a seeding density of  $1 \times 10^5$  cells per well. These cells were treated with 100 nM phorbol-12-myristate-13-acetate (Sigma-Aldrich, India) in the cell culture medium overnight at 37 °C, 5% CO<sub>2</sub>. Afterward, either test samples (0–300 µg mL<sup>-1</sup>) or doxorubicin (0–10 µg mL<sup>-1</sup>) were added to each well and incubated for an additional 48 h at 37 °C. Finally, 5 mg mL<sup>-1</sup> of MTT (20 µL) dye (Sigma-Aldrich) was added to each well, and incubated for an additional 4 h at 37 °C, 5% CO<sub>2</sub>. The absorbance at 570 nm was measured using a microplate reader (Molecular Devices, USA) and the percentage inhibition and IC<sub>50</sub> values of THP-1 macrophages was determined accordingly.

### Molecular docking studies

All four isolated secondary metabolites (fukinanolide A, pinastric acid, stictic acid, and scrobiculin) were docked into published X-ray crystal structures of essential TB enzymes using AutoDock v4.2, as previously reported.<sup>47–49</sup> Crystal structure of 14 $\alpha$ -sterol demethylase cytochrome P450 (PDB ID: 1EA1),<sup>50</sup> mycobacterial ATP synthase (PDB ID: 4V1F),<sup>37</sup> and  $\beta$ -ketoacyl reductase FabG4 (PDB ID: 3V1U)<sup>30</sup> from *M.tb* were selected for molecular docking study by rationalizing the ligand similarity and site of action.<sup>51</sup> The X-ray crystal structures of these proteins were retrieved from RCSB website<sup>52</sup> to generate initial 3D coordinates. The docking protocols were validated by redocking the co-crystal ligands into their respective receptors (Fig. 2A–C).<sup>53</sup> The receptor proteins were prepared by removing the co-crystallised water molecules, and then polar hydrogens were added. Gasteiger charges were added for ligand and receptor atoms, and atomic radii were specified for each system, along with AutoDock4 atom types as described earlier.<sup>48,49</sup> A grid map for each compound was created over the native ligand position in the binding site. Finally, grid parameter file (.gpf) and docking parameter files (.dpf) were run using Lamarckian algorithm.<sup>54</sup> In order to gain further insight into binding mode and interaction of the compound with the different receptors, MGL tools were employed.<sup>47</sup>

### Conclusions

In conclusion, this study provides the initial evidence confirming the existence of antimycobacterial secondary metabolites in *L. pulmonaria*. The bioassay-guided isolation of LP metabolites identified potent anti-MDR-tubercular agents. The REMA screening showed that stictic acid and fukinanolide A exhibit significantly high inhibitory effects against six MDR-TB isolates, compared to rifampicin. Additionally, MTT assay and SI ration allowed us to understand the less cytotoxicity nature of stictic acid and fukinanolide A, compared to rifampicin.

Molecular docking studies further suggested that the principal mode of action of stictic acid and fukinanolide A involve the inhibition of cytochrome P450 14 $\alpha$ -sterol demethylase and  $\beta$ -ketoacyl reductase, thereby compromising mycobacterial cell wall integrity, fatty acid metabolism, and survival. Our data strongly support the antimicrobial potential of stictic acid and fukinanolide A combination and/or with standard anti-TB drugs, as suitable candidates for the next generation of MDR-TB drugs. The limitation of the current study includes lack of *in vivo* investigations to confirm the efficacy and safety of *L. pulmonaria* extracts and isolated compounds. Future studies involving animal models are necessary to assess pharmacokinetics, bioavailability, and toxicity, thereby validating the therapeutic potential of *L. pulmonaria* against TB.

### Author contributions

HTN and VBT conceived the study and analysed the data. HP, EO, and NHT conducted *in vitro* antimycobacterial studies and cytotoxicity studies. VNB, SM, WMNHWS and RAB performed docking studies. All authors co-wrote and reviewed the manuscript.

### Conflicts of interest

There are no conflicts to declare.

### Data availability

All the data supporting this article have been included in the manuscript.

Supplementary information (SI): all spectral data for the isolated compound. See DOI: <https://doi.org/10.1039/d5ra05774d>.

### References

- 1 C. Lienhardt, P. Glaziou, M. Uplekar, K. Lönnroth, H. Getahun and M. Raviglione, *Nat. Rev. Microbiol.*, 2012, **10**, 407–416.
- 2 K. Lönnroth, K. G. Castro, J. M. Chakaya, L. S. Chauhan, K. Floyd, P. Glaziou and M. C. Raviglione, *Lancet*, 2010, **375**, 1814–1829.
- 3 World Health Organization, *Global tuberculosis report 2023*, Geneva, 2023.
- 4 World Health Organization, *Global tuberculosis report 2024*, Geneva, 2024.
- 5 I. Barilar, T. Fernando, C. Utpatel, C. Abujate, C. M. Madeira, B. José, C. Mutaquiha, K. Kranzer, T. Niemann, N. Ismael, L. de Araujo, T. Wirth, S. Niemann and S. Viegas, *Lancet Infect. Dis.*, 2023, **24**, 297–307.
- 6 A. K. Verma, R. N. Yadav, G. Kumar and R. K. Dewan, *J. Clin. Tuberc. Other Mycobact. Dis.*, 2022, **27**, 100317.
- 7 J. Cameron, *The Gaelic names of plants*, John MacKay, Glasgow, 1900, 2nd edn.



- 8 R. De Crespigny and H. Hutchinson, *The new forest: Its traditions, inhabitants and customs*, John Murray, London, 1903.
- 9 J. Pereira, London, 1850.
- 10 S. Watson, *Philos. Trans. R. Soc. London*, 1756, **49**, 803–806.
- 11 J. R. C. Wise, *The New Forest: Its history and its scenery*, Smith, Elder, and Co., London, 1863.
- 12 Lichens Used in Traditional Medicine, in *Lichen Secondary Metabolites*, Springer International Publishing, Cham, 2015, pp. 27–80, DOI: [10.1007/978-3-319-13374-4\\_2](https://doi.org/10.1007/978-3-319-13374-4_2).
- 13 D. K. Upreti, R. Bajpai and S. Nayaka, *Plant Biology and Biotechnology*, Springer India, New Delhi, 2015, pp. 263–280.
- 14 M. X. Yang, S. Devkota, L. S. Wang and C. Scheidegger, *Diversity*, 2021, **13**, 330.
- 15 K. O. Vartia, *The Lichens*, Elsevier, 1973, pp. 547–561.
- 16 F. Atalay, F. Odabasoglu, M. Halici, A. Cakir, E. Cadirci, A. Aslan, O. A. Berktaş and C. Kazaz, *Chem. Biodivers.*, 2015, **12**, 1756–1767.
- 17 B. Goncu, E. Sevgi, C. K. Hancer, G. Gokay and N. Ozten, *PLoS One*, 2020, **15**, e0238303.
- 18 B. Karakus, F. Odabasoglu, A. Cakir, Z. Halici, Y. Bayir, M. Halici, A. Aslan and H. Suleyman, *Phytother Res.*, 2009, **23**, 635–639.
- 19 M. Kello, M. Goga, K. Kotorova, D. Sebova, R. Frenak, L. Tkacikova and J. Mojzis, *Plants*, 2023, **12**, 611.
- 20 B. Pejcin, G. Tommonaro, C. Iodice, V. Tesevic and V. Vajs, *Nat. Prod. Res.*, 2012, **26**, 1634–1637.
- 21 S. Salem, E. Leghouchi, R. Soulimani and J. Bouayed, *Int. J. Vitam. Nutr. Res.*, 2019, **91**, 143–151.
- 22 H. Süleyman, F. Odabasoglu, A. Aslan, A. Cakir, Y. Karagoz, F. Gocer, M. Halici and Y. Bayir, *Phytomedicine*, 2003, **10**, 552–557.
- 23 T. J. Nolan and J. Keane, *Nature*, 1933, **132**, 281.
- 24 B. Pejcin, G. Tommonaro, C. Iodice, V. Tesevic, V. Vajs and S. De Rosa, *J. Enzyme Inhib. Med. Chem.*, 2013, **28**, 876–878.
- 25 C. F. Culbertson, *Bryologist*, 1969, **72**, 19–27.
- 26 F. Atalay, M. B. Halici, A. Mavi, A. Cakir, F. Odabaşoğlu, C. Kazaz, A. Aslan and Ö. I. Küfrevioğlu, *Turk. J. Chem.*, 2011, **35**, 647–661.
- 27 B. Pejcin, C. Iodice, G. Bogdanović, V. Kojić and V. Tešević, *Arab. J. Chem.*, 2017, **10**, S1240–S1242.
- 28 A. Rassabina, V. Khabibrakhmanova, V. Babaev, A. Daminova and F. Minibayeva, *Int. J. Mol. Sci.*, 2022, **23**, 15605.
- 29 D. R. Banerjee, K. Senapati, R. Biswas, A. K. Das and A. Basak, *Bioorg. Med. Chem. Lett.*, 2015, **25**, 1343–1347.
- 30 D. Dutta, S. Bhattacharyya, A. Roychowdhury, R. Biswas and A. K. Das, *Biochem. J.*, 2013, **450**, 127–139.
- 31 Z. Q. Xu, W. W. Barrow, W. J. Suling, L. Westbrook, E. Barrow, Y. M. Lin and M. T. Flavin, *Bioorg. Med. Chem.*, 2004, **12**, 1199–1207.
- 32 V. K. Gupta, A. Kaushik, D. S. Chauhan, R. K. Ahirwar, S. Sharma and D. Bisht, *J. Ethnopharmacol.*, 2018, **227**, 113–120.
- 33 N. B. Bapela, N. Lall, P. B. Fourie, S. G. Franzblau and C. E. J. Van Rensburg, *Phytomedicine*, 2006, **13**, 630–635.
- 34 J. P. Dzoyem, A. O. Aro, L. J. McGaw and J. N. Eloff, *S. Afr. J. Bot.*, 2016, **102**, 70–74.
- 35 H. Li and T. L. Poulos, *Nat. Struct. Biol.*, 1997, **4**, 140–146.
- 36 G. M. Courbon, P. R. Palme, L. Mann, A. Richter, P. Imming and J. L. Rubinstein, *EMBO J.*, 2023, **42**, e113687.
- 37 L. Preiss, J. D. Langer, Ö. Yildiz, L. Eckhardt-Strelau, J. E. Guillemont, A. Koul and T. Meier, *Sci. Adv.*, 2015, **1**, e1500106x.
- 38 D. Matthies, W. Zhou, A. L. Klyszejko, C. Anselmi, Ö. Yildiz, K. Brandt, V. Müller, J. D. Faraldo-Gómez and T. Meier, *Nat. Commun.*, 2014, **5**, 5286.
- 39 D. Pogoryelov, A. Krah, J. D. Langer, Ö. Yildiz, J. D. Faraldo-Gómez and T. Meier, *Nat. Chem. Biol.*, 2010, **6**, 891–899.
- 40 E. M. Cross, F. G. Adams, J. K. Waters, D. Aragão, B. A. Eijkelkamp and J. K. Forwood, *Sci. Rep.*, 2021, **11**, 7050.
- 41 V. Gerusz, *Annu. Rep. Med. Chem.*, 2010, **45**, 295–311.
- 42 E. Poulsen-Silva, M. C. Otero, S. Diaz-Cornejo, C. Atala, J. A. Fuentes and F. Gordillo-Fuenzalida, *Fungal Biol. Rev.*, 2025, **51**, 100410.
- 43 V. B. Tatipamula and S. S. P. Annam, *J. Ethnopharmacol.*, 2022, **282**, 114641.
- 44 S. Huneck and I. Yoshimura, *Identification of Lichen Substances*, Springer Berlin Heidelberg, 1996, pp. 11–123.
- 45 N. H. Thuan, H. Polimati, R. Alluri and V. B. Tatipamula, *3 Biotech*, 2022, **12**, 95.
- 46 B. R. Chitturi, D. B. Chanti, V. B. Tatipamula, S. Dudem, S. V. Kalivend, V. R. Tuniki, A. B. Richard and V. Yenamandra, *Nat. Prod. Res.*, 2015, **29**, 70–76.
- 47 G. M. Morris, R. Huey, W. Lindstrom, M. F. Sanner, R. K. Belew, D. S. Goodsell and A. J. Olson, *J. Comput. Chem.*, 2009, **30**, 2785–2791.
- 48 V. N. Badavath, A. Kumar, P. K. Samanta, S. Maji, A. Das, G. Blum, A. Jha and A. Sen, *J. Biomol. Struct. Dyn.*, 2022, **40**, 3110–3128.
- 49 M. Saravanabhavan, V. N. Badavath, S. Maji, S. Muhammad and M. Sekar, *New J. Chem.*, 2019, **43**, 17231–17240.
- 50 L. M. Podust, T. L. Poulos and M. R. Waterman, *Proc. Natl. Acad. Sci.*, 2001, **98**, 3068–3073.
- 51 J. H. Grosset and R. E. Chaisson, *Handbook of Tuberculosis*, Springer, 2017.
- 52 H. M. Berman, J. WestBrook, Z. Feng, G. Gilliland, T. N. Bhat, H. Weissig, I. N. Shindyalov and P. E. Bourne, *Nucleic Acids Res.*, 2000, **28**, 235–242.
- 53 K. E. Hevener, W. Zhao, D. M. Ball, K. Babaoglu, J. Qi, S. W. White and R. E. Lee, *J. Chem. Inf. Model.*, 2009, **49**, 444–460.
- 54 G. M. Morris, D. S. Goodsell, R. S. Halliday, R. Huey, W. E. Hart, R. K. Belew and A. J. Olson, *J. Comput. Chem.*, 1998, **19**, 1639–1662.

